Numerical analysis of axisymmetric shells by one-dimensional continuum elements suitable for high frequency excitations

Juan José López Cela [a,*], Consuelo Huerta [b], Enrique Alarcón [b]

[a] *Universidad de Castilla-La Mancha, ETS Ingenieros Industriales, Ciudad Real 13071, Spain*
[b] *Universidad Politécnica de Madrid, ETS Ingenieros Industriales, José Gutierrez Abascal 2, 28006 Madrid, Spain*

Abstract

Axisymmetric shells are analyzed by means of one-dimensional continuum elements by using the analogy between the bending of shells and the bending of beams on elastic foundation. The mathematical model is formulated in the frequency domain. Because the solution of the governing equations of vibration of beams are exact, the spatial discretization only depends on geometrical or material considerations. For some kind of situations, for example, for high frequency excitations, this approach may be more convenient than other conventional ones such as the finite element method.

Keywords: Axisymmetric shells; Continuum elements; Frequency domain; High frequency excitations

1. Introduction

This work deals with the numerical analysis of axisymmetric shells by means of one-dimensional continuum elements. This is a different approach from that followed in, for example, Refs. [1,2] for static analysis and Ref. [3] for dynamic analysis in which the well-known analogy between the bending of shells and the bending of beams on elastic foundation is used. In these referenced works, a finite element is formulated to analyze the shells: an 'equivalent' finite beam on elastic foundation. The foundation modulus and the beam flexural rigidity are replaced by appropriate parameters pertaining to the shell under consideration. This 'equivalent' finite element formulation avoids two disadvantages in using shell finite elements in computer programs, namely, the higher complexity of shell theories and the greater computational effort the shell elements need, because, they generally have more degrees of freedom.

In the approach proposed in this paper, no finite element is formulated. The development is based on the classical vibration continuum theory, [4,5]. We benefitted from field equation of beams that are solvable with their exact solutions. First, the field equation of a beam for a given frequency is solved and then, by means of the relationships between forces and displacements, the element stiffness matrix for this frequency is obtained. Then, it proceeds like a typical matrix structural analysis scheme. The solution obtained for the entire structure is exact for this frequency because the exact solution of the differential equation of the beam has been previously computed.

An interesting application of this method is the dynamic analysis of structures subjected to high frequency excitations. Because the solution is exact, the spatial discretization may have elements as large as desired being constrained only by the changes of the material properties and the boundary conditions. An example is analyzed in Ref. [6]: the dynamic effects induced in a plane specimen of the ARIANE 5 Vehicle Equipment Bay (A5 VEB) produced by the sudden rupture of the

ring connecting the upper stage of the vehicle by means of a pyrotechnic device. For this case, the mathematical model was built up with continuum beam elements and the numerical results predicted rather good the experimental ones.

In the case of the pyrotechnic shock in the A5 VEB, the frequency contents of the load reaches 30 000 Hz in the structure, while its first natural frequency is about 10 Hz. In this situation, methods based on spatial discretization (for example, the finite element method, FEM) are no longer suitable because they need a very fine mesh and/or very small integration intervals that makes any realistic computational model impractical.

To solve axisymmetric structures, the same approach can be used but by taking into account the beam on elastic foundation analogy. The only difference is that the field equation has changed due to the elastic foundation, but this equation is also solvable and again the solution is exact. Once again, the method can be applied successfully to dynamic analysis. Let us take the case of a cylindrical structure. We can study it (statically or dynamically) with a beam on elastic foundation, but we will focus in the case of dynamics because it highlights the advantages of the method. Using the Finite Element Method some spatial discretization is needed. On the other hand, the higher the range of frequencies, we want to analyze, the higher is the number of elements we need. This, of course, is not critical, even in very big models, for the low frequency regime, due to the current capability of modern computers. But in cases of very high frequency excitations, such as the A5 VEB analysis briefly explained above, the difference in computation time and effort is enormous. Moreover, the complexity of these kind of problems implies a great number of uncertainities both in the definition of the load induced by the pyrotechnic shock and in the modelling of the structure. The only practical way to tackle and solve such a problem is to have at one's disposal a computational method that allows to perform easy and quickly parametric studies with a sufficient confidence. A qualitative study of axisymmetric models of the A5 VEB structures can be found in Refs. [7,8].

In this paper, the mathematical basis of the method is presented, and it is applied to cylindrical and conical structures. Although the formulation has been developed taking into account orthotropic materials, the examples presented in this work are isotropic ones. Other geometrical forms of shells such as hyperboloids can be modelled as an assemblage of conical shell elements [2] and then, can be considered as particular cases of the analyzed ones. In any case, the aim of the paper is not to study many different shapes of shell structures but to show how they can be efficiently calculated by means of a continuum approach.

Because in conical shells one of the radii of curvature is variable some discretization is needed for their modelling. However, this discretization is needed due to the geometry of conical shells and it does not depend on the range of frequencies of interest. We will show in this work that after a certain value of the frequency, the effect of the curvature vanish, i.e. higher values of frequencies of an axisymmetric structure and a plane one (infinite radius) are practically the same. This is a very important phenomenon because it allows us to model a conical shell with just the number of elements needed to predict its behavior up to this value of the frequency. For higher frequencies, the discretization is enough because the circumferential effect has disappeared and the shell behaves like a plane structure that can be modelled by means of continuum beam elements independently of the analyzed range of frequencies.

2. Mathematical model

2.1. Generalities

The mathematical model is formulated in the frequency domain, so it is necessary to compute the structural response for all the harmonic components of the excitation. If the field equation is solvable in the frequency domain, the computation of the impedance matrix is immediate by the application of the proper unit boundary displacements, as it is sketched in Section 2.2. The elements used are beams of the Rayleigh–Timoshenko type, i.e., with axial, shear and bending deformation plus rotational inertia.

To model axisymmetric structures, beams on elastic foundation are used. So, it is necessary to compare their respective field equations to obtain the characteristics of the beams. This is performed in Section 2.3. Once the equivalent beam has been obtained, the computation of the impedance matrix can be carried out.

In the frequency domain it is easy to apply the concept of a complex stiffness incorporating the effects of distributed and/or lumped masses, and elastic (springs) or dissipative elements (dashpots). The lumped masses and the concentrated springs are added directly to the real part of the global impedance matrix $D(\omega)$, while the dashpots affects the imaginary one. By using complex elasticity and shear moduli, it allows the consideration of different damping types: viscous, hysteretic and variable with frequency following a desired law.

Once the global impedance matrix $D(\omega)$ has been assembled, the load vector $F(\omega)$ can be organized for every frequency and the displacement field is obtained by solving

$$x(\omega) = D^{-1}(\omega)F(\omega), \tag{1}$$

$$\dot{x} = \mathrm{i} \cdot \omega x(\omega), \tag{2}$$

$$\ddot{x} = -\omega^2 x(\omega), \tag{3}$$

where ω is the angular frequency and i is the imaginary unit.

The procedure is summarized in Fig. 1. First of all, the frequency history of the load is discretized in a certain number of points. Then the vector of displacements is obtained for each value of the frequency by solving Eq. (1), which gives a discrete curve in the frequency domain for each degree of freedom. The represented magnitudes in the y axis may be displacements, accelerations, forces, etc. The obtained curves are similar to that shown in Fig. 1, the amplifications correspond to the modes and their x values correspond to the natural frequencies (which are independent of the magnitude in the vertical axis). So, the method does not compute neither the frequencies nor the modal shapes. But it is possible to determine where the natural frequencies are by examining the structural response. In the example shown in Fig. 1, with a clamped-free cylinder radially excited, the x values of the peaks are the frequencies of the radial vibration modes. Other modes, like axial or torsional ones, are not present in the response because they have been not excited.

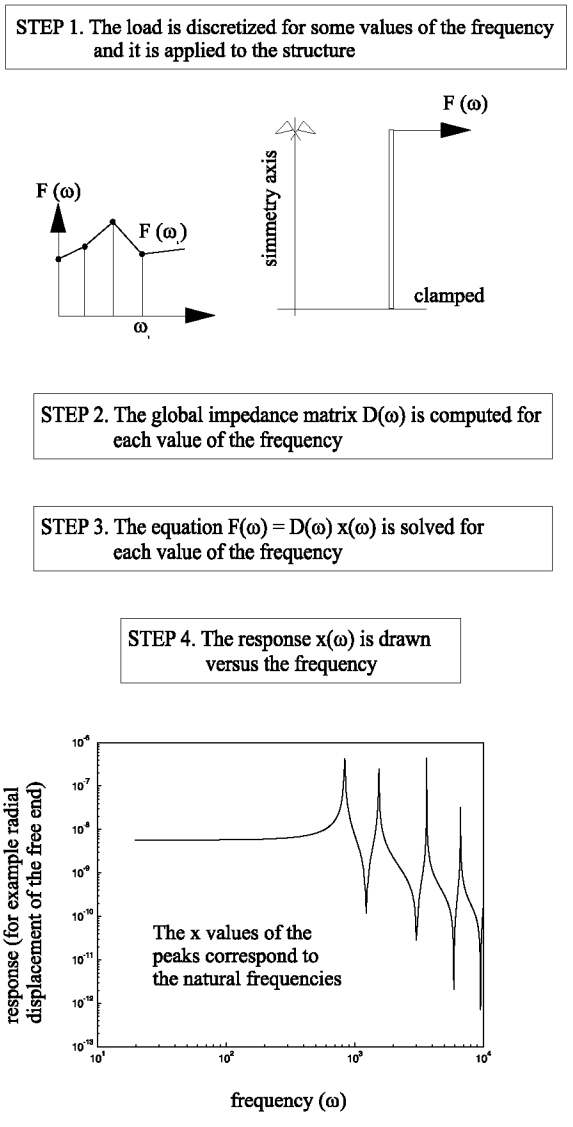

Fig. 1. Schematic representation of the proposed method.

To perform a static calculation, it is only necessary to compute the response for a value of 0 Hz. An inverse Fourier transformation block computes the superposition of the different frequency responses to synthesize the time response. The method also allows for the treatment of load cases with different frequency contents.

The responses are calculated in the nodes of the elements, but to obtain displacements and forces in different points of the elements, the shape functions are used for the interpolation.

2.2. Element impedance matrix

This section illustrates the derivation some of the terms of the dynamic element stiffness matrix in the case of Bernoulli beams, that is, without considering shear deformation. For simplicity, we consider beams of homogeneous material and uniform cross-section. We are looking for an expression of the type,

$$\underline{F^e}(\omega) = \underline{D^e}(\omega)\underline{x^e}(\omega), \tag{4}$$

where $\underline{F^e}(\omega)$ is the element load vector, $\underline{x^e}(\omega)$, the element displacement vector and $\underline{D^e}(\omega)$, the element impedance matrix. The size of the vectors $\underline{F^e}$ and $\underline{x^e}$ is (12×1), whereas the size of $\underline{D^e}(\omega)$ is (12×12).

First of all, we derive the axial terms corresponding to the degree of freedom 1 and 7 (Fig. 2). The field equation of the longitudinal vibration of a beam is

$$EA\frac{\mathrm{d}^2u}{\mathrm{d}x^2} = m\frac{\mathrm{d}^2u}{\mathrm{d}t^2}, \tag{5}$$

where E is Young's modulus, A is the cross-section, m is the mass per unit length and u is the longitudinal displacement.

Because $\mathrm{d}^2u/\mathrm{d}t^2 = -\omega^2 u$, where ω is the angular frequency, the field equation becomes

$$\frac{\mathrm{d}^2u}{\mathrm{d}x^2} + \frac{\omega^2 m}{EA}u = 0. \tag{6}$$

The solution of this equation takes the form,

$$u = C\cos\lambda x + D\sin\lambda x, \tag{7}$$

where C and D are constants and

$$\lambda = \sqrt{\frac{\omega^2 m}{EA}}. \tag{8}$$

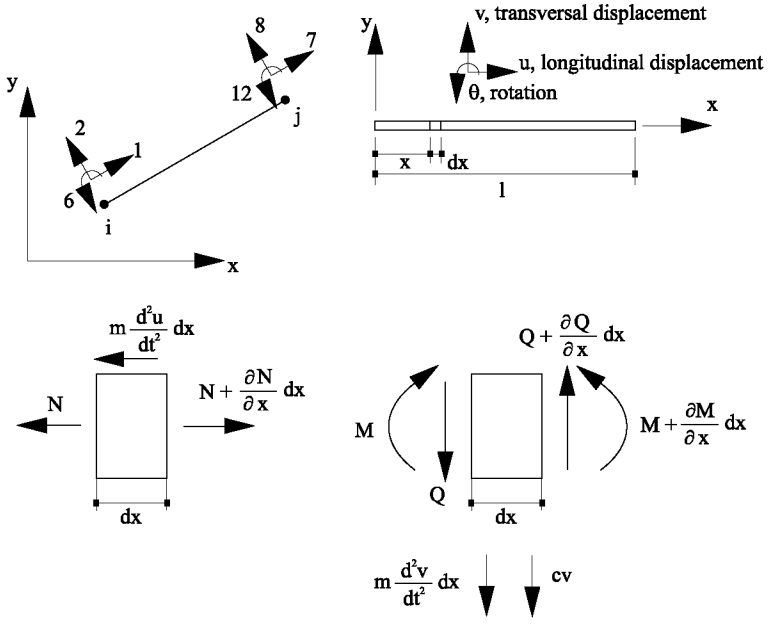

Fig. 2. Sign conventions for displacements and forces.

To obtain the value of the constants the boundary conditions are used: for $x = 0$, (i.e., i end of the beam), $u = u_i$, and for $x = l$, (i.e., j end of the beam) $u = u_j$, so

$$\begin{bmatrix} C \\ D \end{bmatrix} = \begin{bmatrix} 1 & 0 \\ -\cot \lambda l & \frac{1}{\sin \lambda l} \end{bmatrix} \begin{bmatrix} u_i \\ u_j \end{bmatrix}. \tag{9}$$

The relation between axial forces N and axial displacements u is

$$N = EA\frac{\mathrm{d}u}{\mathrm{d}x}, \tag{10}$$

and therefore, particularizing for the ends of the beam, we obtain the longitudinal terms of the impedance matrix. Note that the angular frequency ω is present in λ (Eq. (8)).

$$\begin{bmatrix} N_i \\ N_j \end{bmatrix} = EA\lambda \begin{bmatrix} \cot \lambda l & -\frac{1}{\sin \lambda l} \\ -\frac{1}{\sin \lambda l} & \cot \lambda l \end{bmatrix} \begin{bmatrix} u_i \\ u_j \end{bmatrix}. \tag{11}$$

Next, the bending terms in the xy plane (degree of freedom 2, 6, 8 and 12) are obtained. The equation of transversal vibration of a beam on an elastic foundation is

$$EI_z\frac{\mathrm{d}^4 v}{\mathrm{d}x^4} + cv + m\frac{\partial^2 v}{\partial t^2} = 0, \tag{12}$$

where I_z is the transversal moment of inertia, c is the rigidity per unit length of the elastic foundation and v the transversal displacements.

Because $\mathrm{d}^2 v/\mathrm{d}t^2 = -\omega^2 v$, where ω is the angular frequency, the field equation becomes

$$EI_z\frac{\mathrm{d}^4 v}{\mathrm{d}x^4} + cv - m\omega^2 v = 0. \tag{13}$$

The solution of this equation is of the form

$$v = A\cos \lambda x + B\sin \lambda x + C\cosh \lambda x + D\sinh \lambda x, \tag{14}$$

where A, B, C and D are constants and

$$\lambda^4 = \frac{c - m\omega^2}{EI}. \tag{15}$$

To obtain the value of the constants, the boundary conditions are used: for $x = 0$, $v = v_i$, $\theta = \theta_i$, and for $x = l$, $v = v_j$, $\theta = \theta_j$. Note that for a beam of the Bernoulli type $\theta = \mathrm{d}v/\mathrm{d}x$, so

$$\begin{bmatrix} A \\ B \\ C \\ D \end{bmatrix} = \frac{1}{2\Delta} \begin{bmatrix} (2\Delta + a_1) & a_2 & a_3 & a_4 \\ -a_5 & \frac{2\Delta}{\lambda} - a_6 & a_7 & -a_8 \\ -a_1 & -a_2 & -a_3 & -a_4 \\ a_5 & a_6 & a_7 & a_8 \end{bmatrix} \begin{bmatrix} v_i \\ \theta_i \\ v_j \\ \theta_j \end{bmatrix}, \tag{16}$$

where

$$\Delta = \cos \lambda l \cosh \lambda l - 1, \tag{17}$$

and the values of the constant a_1 to a_8 are given in Appendix A.

The relationships between shear forces Q, bending moments M and transversal displacements v are

$$M = EI_z \frac{d^2 v}{dx^2}, \tag{18}$$

$$Q = -\frac{dM}{dx} = -EI_z \frac{d^3 v}{dx^3}, \tag{19}$$

and therefore, particularizing for the ends of the beam, we obtain the bending terms of the element impedance matrix

$$\begin{bmatrix} Q_i \\ M_i \\ Q_j \\ M_j \end{bmatrix} = \frac{EI_z}{2\Delta} \begin{bmatrix} 0 & -\lambda^3 & 0 & \lambda^3 \\ \lambda^2 & 0 & -\lambda^2 & 0 \\ -\lambda^3 \sin \lambda l & \lambda^3 \cos \lambda l & -\lambda^3 \sinh \lambda l & -\lambda^3 \cosh \lambda l \\ -\lambda^2 \cos \lambda l & -\lambda^2 \sin \lambda l & \lambda^2 \cosh \lambda l & \lambda^2 \sinh \lambda l \end{bmatrix} \times \begin{bmatrix} (2\Delta + a_1) & a_2 & a_3 & a_4 \\ -a_5 & \frac{2\Delta}{\lambda} - a_6 & a_7 & -a_8 \\ -a_1 & -a_2 & -a_3 & -a_4 \\ a_5 & a_6 & a_7 & a_8 \end{bmatrix} \begin{bmatrix} v_i \\ \theta_i \\ v_j \\ \theta_j \end{bmatrix}. \tag{20}$$

Again, the parameter λ (Eq. (15)) contains the angular frequency ω. The bending terms in the plane xz (degree of freedom 3, 5, 9 and 11) are the same by changing the moment of inertia and the torsional terms (degree of freedom 4 and 10) are obtained like the axial ones.

The derivation of the terms including shear deformation plus rotatory inertia is a little more complicated and can be found in Refs. [5,8] for the case of a beam on elastic foundation.

After the element matrix is computed, it is possible to compose the global impedance matrix $\underline{D}(\omega)$ and to solve Eq. (4) for each discrete value of the frequency.

2.3. Axisymmetric effects

Now, the main characteristics of the behavior of orthotropic axisymmetric shells are presented. The objective is to model axisymmetric structures with the described elements: beams on elastic foundation and springs. Thus, no real extension to two-dimensional elements is performed in the study. Once the characteristics of the equivalent beam have been obtained the computation of the element impedance matrix $\underline{D}^e(\omega)$ can be carried out by applying the expressions of the previous section.

The structure under consideration is a shell with axial symmetry. In Fig. 3, a spherical shell is represented where the meridional and circumferential radii are the same $r_1 = r_2$. The analysis is limited to the case of infinite meridional curvature ($r_1 = \infty$), i.e., only cylindrical

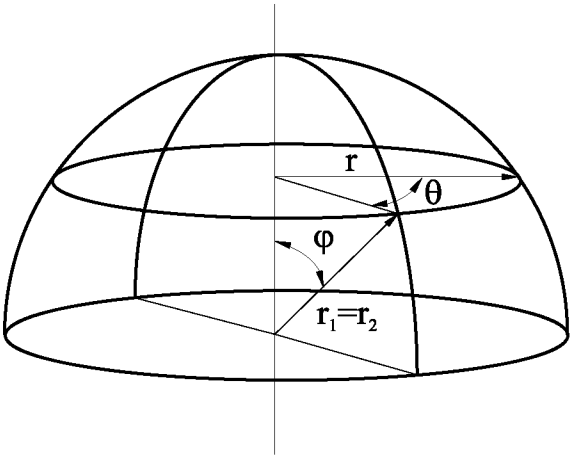

Fig. 3. Thin shell with axial symmetry: definition of the geometry.

($\varphi = 90°$) and conical shells ($\varphi \neq 90°$) are considered, but other kinds of shells such as hyperboloids can be modeled as an assemblage of conical shell elements.

2.3.1. Material behavior law

In the following, subscripts s and θ refer to meridional and circumferential components respectively, while z represents the coordinate normal to the shell plane.

If an orthotropic material is considered, the material behavior law is given by the following relations:

$$\sigma_s = \frac{E_s}{1 - \nu_s \nu_\theta} (\varepsilon_s + \nu_s \varepsilon_\theta), \tag{21}$$

$$\sigma_\theta = \frac{E_\theta}{1 - \nu_s \nu_\theta} (\varepsilon_\theta + \nu_s \varepsilon_s), \tag{22}$$

$$\tau_{sz} = G_{sz} \gamma_{sz}. \tag{23}$$

2.3.2. Kinematic relations

Equations relating displacements with strains in the middle plane of the shell are established. The displacements are defined by means of the meridional u, circumferential v and normal w components as shown in Fig. 4 where positive values have been represented. The assumed displacement model is that of Fig. 5. A fiber of the shell located at z suffers a global translation plus another one due to the rotation α of the normal to the shell plane

$$u = u_0(s) - \alpha(s) z, \tag{24}$$

$$v = 0, \tag{25}$$

$$w = w_0(s), \tag{26}$$

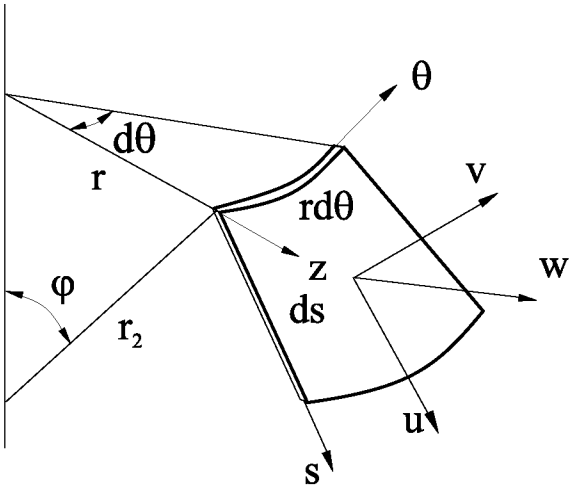

Fig. 4. Definition of displacements in axisymmetric shells.

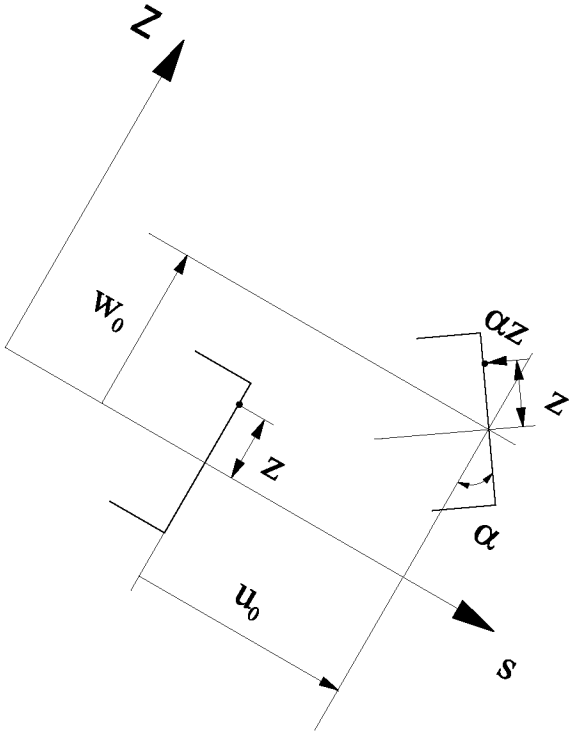

Fig. 5. Assumed displacement model for axisymmetric shells.

where the subscript 0 refers to the displacements in the middle plane of the shell.

The strain along the meridian is

$$\varepsilon_s = \frac{\mathrm{d}u_0}{\mathrm{d}s} - z\frac{\mathrm{d}\alpha}{\mathrm{d}s}, \tag{27}$$

while the strain along the circumferential direction depends on both u and w

$$\varepsilon_\theta = \frac{1}{r_2}(w_0 + u_0 \cot\varphi - \alpha z \cot\varphi) \tag{28}$$

and the angular strain is

$$\gamma_{sz} = -\alpha + \frac{\mathrm{d}w}{\mathrm{d}s}. \tag{29}$$

2.3.3. Equilibrium equations

The equilibrium equations are written by using the principle of virtual work

$$\int_\Omega \underset{\sim}{\sigma} : \delta\underset{\sim}{\varepsilon}\,\mathrm{d}V = \int_\Omega X\delta u\,\mathrm{d}V + \int_{\partial\Omega} \overline{X}\delta u\,\mathrm{d}A, \tag{30}$$

where Ω is the body domain and $\partial\Omega$ is its boundary. X and $\overline{X}$ represent vectors containing the body and surface forces respectively.

For axisymmetric shells, the integral on the volume can be written as

$$\int_\Omega \mathrm{d}V = \int_0^{2\pi}\int_{s_1}^{s_2}\int_{-h}^{h} r\,\mathrm{d}\theta\,\mathrm{d}s\,\mathrm{d}z, \tag{31}$$

where $2h$ is the thickness of the shell.

A general formulation, including shear deformation is studied; therefore the angular strain γ_{sz} is non zero and $\alpha \neq \mathrm{d}w/\mathrm{d}s$.

Neglecting body forces, it is only necessary to consider the surface forces p_s, p_z and m (p_θ is zero because of the symmetry), and then Eq. (31) becomes

$$\begin{aligned}&\int_{s_1}^{s_2}\int_{-h_s}^{h_s} r\sigma_s\,\delta\varepsilon_s\,\mathrm{d}s\,\mathrm{d}z + \int_{s_1}^{s_2}\int_{-h_\theta}^{h_\theta} r\sigma_\theta\,\delta\varepsilon_\theta\,\mathrm{d}s\,\mathrm{d}z\\ &\quad+\int_{s_1}^{s_2}\int_{-h_s}^{h_s} r\tau_{sz}\,\delta\gamma_{sz}\,\mathrm{d}s\,\mathrm{d}z\\ &\quad=\int_{s_1}^{s_2} p_s r\,\delta u\,\mathrm{d}s + \int_{s_1}^{s_2} p_z r\,\delta w\,\mathrm{d}s + \int_{s_1}^{s_2} mr\,\delta\alpha\,\mathrm{d}s.\end{aligned} \tag{32}$$

For the case studied in this work, the surface forces are those due to the inertia effects. Because we are looking for the response of a pure harmonic excitation, the solution can be computed for each frequency, obtaining the spatial distribution of the variables.

2.3.4. Field equations

Two different thicknesses $2h_s$ and $2h_\theta$ are used for the treatment of the orthotropy. Introducing the kinematic relations Eqs. (27)–(29) in Eq. (32), integrating this last equation and splitting the variations of the displacements δu, δw and $\delta\alpha$, the following expressions are obtained:

$$-\frac{\mathrm{d}}{\mathrm{d}s}\left[r\int_{-h_s}^{h_s}\sigma_s\,\mathrm{d}z\right] + \frac{r}{r_2}\cot\varphi\left[\int_{-h_\theta}^{h_\theta}\sigma_\theta\,\mathrm{d}z\right] = p_s r, \tag{33}$$

$$\frac{r}{r_2}\int_{-h_s}^{h_s}\sigma_\theta\,\mathrm{d}z-\frac{\mathrm{d}}{\mathrm{d}s}\left[r\int_{-h_s}^{h_s}\tau_{sz}\,\mathrm{d}z\right]=p_z r, \tag{34}$$

$$-\frac{\mathrm{d}}{\mathrm{d}s}\left[r\int_{-h_s}^{h_s}-z\sigma_s\,\mathrm{d}z\right]+\frac{r}{r_2}\cot\varphi\left[\int_{-h_\theta}^{h_\theta}-z\sigma_\theta\,\mathrm{d}z\right]+r\int_{-h_s}^{h_s}\tau_{sz}\,\mathrm{d}z=mr. \tag{35}$$

The forces per unit length are usually interpreted as the stress resultants, so, using Eqs. (33)–(35),

$$N_s=\int_{-h_s}^{h_s}\sigma_s\,\mathrm{d}z=\frac{E_sA_s}{1-v_sv_\theta}\left[\frac{\mathrm{d}u_0}{\mathrm{d}s}+\frac{1}{r_2}v_sw_0+\frac{1}{r_2}v_su_0\cot\varphi\right], \tag{36}$$

$$N_\theta=\int_{-h_\theta}^{h_\theta}\sigma_\theta\,\mathrm{d}z=\frac{E_\theta A_\theta}{1-v_sv_\theta}\left[\frac{1}{r_2}w_0+\frac{1}{r_2}u_0\cot\varphi+v_\theta\frac{\mathrm{d}u_0}{\mathrm{d}s}\right], \tag{37}$$

$$M_s=\int_{-h_s}^{h_s}-z\sigma_s\,\mathrm{d}z=\frac{E_sI_s}{1-v_sv_\theta}\left[\frac{\mathrm{d}\alpha}{\mathrm{d}s}+\frac{1}{r_2}v_s\alpha\cot\varphi\right], \tag{38}$$

$$M_\theta=\int_{-h_\theta}^{h_\theta}-z\sigma_\theta\,\mathrm{d}z=\frac{E_\theta I_\theta}{1-v_sv_\theta}\left[\alpha\frac{1}{r_2}\cot\varphi+v_\theta\frac{\mathrm{d}\alpha}{\mathrm{d}s}\right], \tag{39}$$

$$Q_{sz}=\int_{-h_s}^{h_s}\tau_{sz}\,\mathrm{d}z=G_{sz}A_{sz}\left[\frac{\mathrm{d}w_0}{\mathrm{d}s}-\alpha\right], \tag{40}$$

where A_s and A_θ are the cross-sections normal to the meridional and circumferential directions respectively, I_s and I_θ are the corresponding moments of inertia and A_{sz} is the shear area. All these characteristics are per unit length.

Eliminating $(\mathrm{d}u_0/\mathrm{d}s)$ from Eqs. (36) and (37) and $(\mathrm{d}\alpha/\mathrm{d}s)$ from Eqs. (38) and (39), it is possible to write the circumferential axial force N_θ and the bending moment M_θ in function of the meridional ones N_s and M_s

$$N_\theta=\frac{E_\theta A_\theta}{r_2}(w_0+u_0\cot\varphi)+v_\theta\frac{E_\theta A_\theta}{E_sA_s}N_s, \tag{41}$$

$$M_\theta=\frac{E_\theta I_\theta}{r_2}\alpha\cot\varphi+v_\theta\frac{E_\theta I_\theta}{E_sI_s}M_s. \tag{42}$$

Substituting the previous equations in Eqs. (33)–(35), the field equations obtained are

$$-\frac{1}{r}\frac{\mathrm{d}}{\mathrm{d}s}\left[K_sr\left(\frac{\mathrm{d}u_0}{\mathrm{d}s}+\frac{1}{r_2}v_sw_0+\frac{1}{r_2}v_su_0\cot\varphi\right)\right]+\frac{E_\theta A_\theta}{r_2^2}\cot^2\varphi(u_0+w_0\tan\varphi)=p_s-v_\theta\frac{K_\theta}{K_s}\frac{\cot\varphi}{r_2}N_s, \tag{43}$$

$$\frac{E_\theta A_\theta}{r_2^2}(w_0+u_0\cot\varphi)-G_{sz}A_{sz}\left[\frac{\mathrm{d}^2w_0}{\mathrm{d}s^2}-\frac{\mathrm{d}\alpha}{\mathrm{d}s}\right]=p_z-v_\theta\frac{K_\theta}{K_s}\frac{1}{r_2}N_s, \tag{44}$$

$$D_s\frac{\mathrm{d}^2\alpha}{\mathrm{d}s^2}+D_s\frac{v_s}{r_2}\alpha\cot\varphi\frac{\mathrm{d}\alpha}{\mathrm{d}s}+G_{sz}A_{sz}\left[\frac{\mathrm{d}w_0}{\mathrm{d}s}-\alpha\right]=\frac{1}{r_2}\cot\varphi\left[\frac{E_\theta I_\theta}{r_2}\alpha\cot\varphi+v_\theta\frac{E_\theta I_\theta}{E_sA_s}M_s\right]-m, \tag{45}$$

where the following notation has been adopted.

$$K_s=\frac{E_sA_s}{1-v_sv_\theta},\qquad K_\theta=\frac{E_\theta A_\theta}{1-v_sv_\theta},$$
$$D_s=\frac{E_sI_s}{1-v_sv_\theta},\qquad D_\theta=\frac{E_\theta I_\theta}{1-v_sv_\theta}.$$

2.4. Approximation of the field equations of cylindrical and conical shells with field equations of beams

The general field equations given by expressions (43)–(45) will be particularized for cylindrical and conical shells and then compared to the field equations of beams, in order to establish the conditions under which axisymmetric shells can be modeled by beams.

2.4.1. Cylindrical shells

The longitudinal behavior, described by Eq. (43) can be particularized for a cylinder shell taking into account that in this case $\varphi=90^\circ$ and therefore $r=r_2=R=$ constant.

$$-K_s\frac{\mathrm{d}^2u_0}{\mathrm{d}s^2}=p_s+\frac{v_s}{R}\frac{\mathrm{d}}{\mathrm{d}s}(K_sw_0). \tag{46}$$

Eq. (46) is the field equation of the axial behavior of a bar if the last term (coupling between axial and bending behavior) is neglected. This approximation is valid for short cylinders for which axisymmetric effects are important.

The transversal behavior is defined by Eqs. (44) and (45).

$$\frac{E_\theta A_\theta}{R^2}w-G_{sz}A_{sz}\left(\frac{\mathrm{d}^2w_0}{\mathrm{d}s^2}-\frac{\mathrm{d}\alpha}{\mathrm{d}s}\right)=p_z-\frac{v_\theta}{R}\frac{K_\theta}{K_s}N_s, \tag{47}$$

$$D_s\frac{\mathrm{d}^2\alpha}{\mathrm{d}s^2}+G_{sz}A_{sz}\left(\frac{\mathrm{d}w_0}{\mathrm{d}s}-\alpha\right)=-m. \tag{48}$$

Eqs. (47) and (48) (if we neglect the coupling with the axial behavior), are equivalent to those of a beam on elastic foundation of stiffness,

$$k = \frac{E_\theta A_\theta}{R^2}. \tag{49}$$

The transversal moment of inertia of the beam is

$$I = \frac{I_s}{1 - \nu_s \nu_\theta}, \tag{50}$$

and Young's modulus,

$$E = E_s. \tag{51}$$

2.4.2. Conical shells

For the case of conical shells we use the hypothesis of Geckeler that proposes to take into account only the terms with the highest derivative. Therefore, Eqs. (43), (44) and (56) become

$$-K_s \frac{d^2 u_0}{ds^2} + \frac{E_\theta A_\theta}{r_2^2} \cot^2 \varphi (u_0 + w_0 \tan \varphi) = p_s - \nu_\theta \frac{K_\theta}{K_s} \frac{\cot \varphi}{r_2} N_s + \frac{\nu_s}{r_2} K_s \frac{dw_0}{ds}, \tag{52}$$

$$\frac{E_\theta A_\theta}{r_2^2}(w_0 + u_0 \cot \varphi) - G_{sz} A_{sz} \left[\frac{d^2 w_0}{ds^2} - \frac{d\alpha}{ds} \right] = p_z - \nu_\theta \frac{K_\theta}{K_s} \frac{1}{r_2} N_s, \tag{53}$$

$$D_s \frac{d^2 \alpha}{ds^2} + G_{sz} A_{sz} \left[\frac{dw_0}{ds} - \alpha \right] = \frac{1}{r_2} \cot \varphi \left[\frac{E_\theta I_\theta}{r_2} \alpha \cot \varphi + \nu_\theta \frac{E_\theta I_\theta}{E_s A_s} M_s \right] - m. \tag{54}$$

The last term of Eq. (52) can be neglected if $dw_0/ds < d^2 u_0/ds^2$. We can see that expressions (52), (53) and (37) correspond to the field equations of a beam except for the terms $(E_\theta A_\theta / r_2^2) \cot^2 \varphi (u_0 + w_0 \tan \varphi)$ in Eq. (52) and $(E_\theta A_\theta / r_2^2)(w_0 + u_0 \cot \varphi)$ in Eq. (53), that is, coupling between the longitudinal and transversal displacements due to the slope of the shell. This effect can be represented by means of a beam supported on concentrated springs normal to the axis of the cone. The force exerted for the spring due to the displacement w is $F = Kw \sin \varphi$ while that due to u is $F = Ku \cos \varphi$ (Fig. 6). Adding the two effects

$$F_w = -K \sin \varphi (w_0 \sin \varphi + u_0 \cos \varphi) = -K(u_0 \sin \varphi \cos \varphi + w_0 \sin^2 \varphi), \tag{55}$$

$$F_s = -K \cos \varphi (w_0 \sin \varphi + u_0 \cos \varphi) = -K(u_0 \cos^2 \varphi + w_0 \sin \varphi \cos \varphi), \tag{56}$$

where subscript w refers to the bending terms and s to the axial ones. If we take

$$K = \frac{E_\theta A_\theta}{r_2^2 \sin^2 \varphi}, \tag{57}$$

we obtain

$$F_w = -\frac{E_\theta A_\theta}{r_2^2}(u \cot \varphi + w), \tag{58}$$

$$F_s = -\frac{E_\theta A_\theta}{r_2^2} \cot^2 \varphi (u + w \tan \varphi), \tag{59}$$

that are, respectively, the added terms in the previous equations. In these equations, r_2 represents an average radius between the radii corresponding to the ends of the beam.

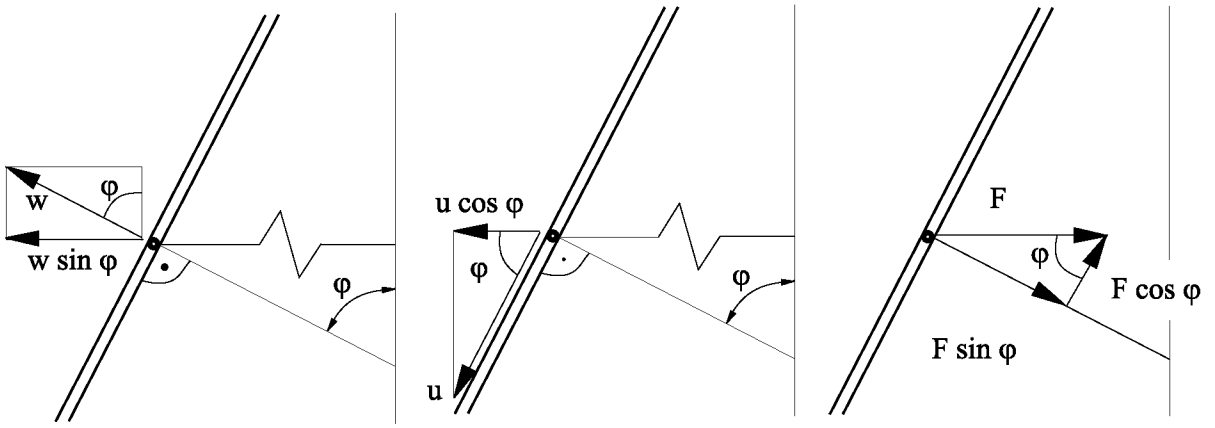

Fig. 6. Modeling for conical shells.

3. Application examples

3.1. Validation examples

In this section, we validate the proposed method by comparing some results with finite element calculations. Two clamped-free cylinders and cones of different lengths and isotropic materials are studied. The geometrical and material characteristics are indicated in Table 1. The compared magnitudes are natural frequencies of radial modes and element forces per unit length due to static radial loads, i.e., dynamic computations for 0 Hz. The finite element models are built up with two-node axisymmetric shell elements. In particular, the SHELL61 element of the well-known ANSYS code [9] is used.

For the proposed method, it is necessary to obtain the characteristics of the equivalent one-dimensional continuum structures according to Section 2.

Cylindrical structures are modeled by an equivalent beam on elastic foundation with the following characteristics:

$$E = E_s = 7 \times 10^{10}\ \mathrm{N/m^2}.$$

Taking into account that the radius is constant, the area of the cross-section of the equivalent beam, for a depth of $b = 1$ m, is

$$A = A_\theta = tb = 1 \times 10^{-2}\ \mathrm{m^2}$$

and the moment of inertia and stiffness modulus are

$$I = \frac{I_s}{1 - v_s v_\theta} = \frac{1}{1 - 0.09}\frac{1}{12}\left(1 \times 10^{-2}\right)^3 = 9.15 \times 10^{-8}\ \mathrm{m^4},$$

$$k = \frac{E_\theta A_\theta}{R^2} = \frac{7 \times 11^{10} \times 1 \times 10^{-2}}{1^2} = 7 \times 10^8\ \mathrm{N/m^2}.$$

Conical structures are modeled by beams on concentrated springs normal to the axis of the cone. The values of the transversal section, the moment of inertia and the stiffness of the concentrated springs vary along the axis of the cone, because the depth b is not constant. The springs are located between two elements and their stiffnesses are

$$K = \frac{E_\theta A_\theta tb}{(r_2 \sin\varphi)^2}\frac{L_1 + L_2}{2},$$

where L_1 and L_2 are the lengths of the two beam elements before and after the spring and the radius r_2 is that corresponding to the location of the spring.

In Table 2, the values of the first five radial natural frequencies obtained with both calculations are shown. The finite element code uses a standard modal analysis (Ref. [9]), but it is important to highlight again that the proposed method does not compute neither the frequencies nor the modal shapes but the structural response, for certain values of frequency, produced by an external excitation.

In Fig. 7, a typical response history in the frequency domain is shown. In particular, the radial displacement of the free end of cylinder 2 is plotted. The external excitation is a step load applied in the radial direction on the free edge of the cylinder. The values of the x coordinates of the peaks (838, 1572, 3804 and 6743 Hz) correspond to the natural frequencies. These values are compared with the natural frequencies obtained with the finite element computation (843, 1546, 3648 and 6659 Hz).

The range of analyzed frequencies for cylinders is from 0 to 10 000 Hz and the number of calculated frequencies is 512, i.e., the response is computed for each of 19.53 Hz. For cones also, 512 frequencies have been

Table 1
Validation examples – geometrical and material characteristics

	Cylinder 1	Cylinder 2	Cone 1	Cone 2
R_{max} (m)	1	1	2	2
R_{min} (m)	1	1	1	1
Length (m)	1	0.2	1	0.2
Thickness (m)	1×10^{-2}	1×10^{-2}	1×10^{-2}	1×10^{-2}
ρ (kg/m^3)	2700	2700	2700	2700
E (N/m^2)	7×10^{10}	7×10^{10}	7×10^{10}	7×10^{10}
v	0.3	0.3	0.3	0.3

Table 2
Validation examples: comparison of axisymmetric (radial) frequencies

Mode	Cylinder 1		Cylinder 2		Cone 1		Cone 2	
	Continuum–FEM	Error (%)	Continuum–FEM	Error (%)	Continuum–FEM	Error (%)	Continuum–FEM	Error (%)
1	792–795	0.3	838–843	0.5	275–286	4	78–82	5
2	810–810	0	1572–1546	1	320–330	3	109–111	1.8
3	821–823	0.2	3804–3648	4	371–379	2	180–180	0.1
4	861–862	0.1	6743–6695	7	422–429	1.5	305–305	0.1
5	946–943	0.3	No data	–	477–483	1.2	485–484	0.2

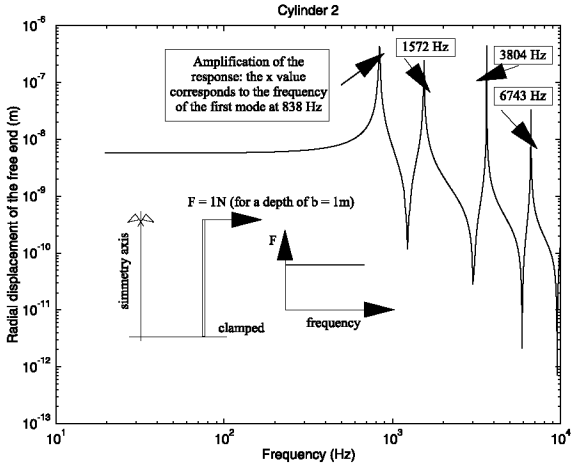

Fig. 7. Typical response history in the frequency domain and radial displacement of free end for cylinder 2.

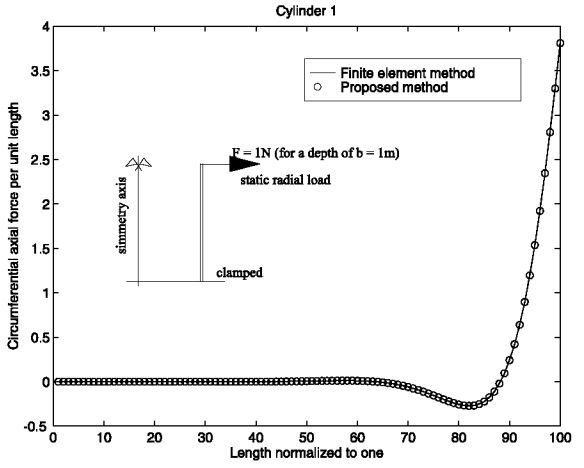

Fig. 8. Validation examples for cylinder 1 and circumferential axial force per unit length and static radial load.

Table 3
Validation examples: number of nodes and elements

	Cylinders		Cones	
	Continuum	FEM	Continuum	FEM
Nodes	2	101	21	101
Elements	1	100	20	100

calculated, but in these cases, the range is from 0 to 5000 Hz.

In Table 3, the number of nodes and elements used in both mathematical models are shown. Note that for cylinders, one element is necessary to capture all the frequencies with the proposed method. The current finite element discretization is valid for certain number of modes. After a determined threshold, a finer mesh should be needed. However, the continuum method does not need more than one element, with the corresponding savings in computation time.

For the cases of cones, some discretization is needed because the characteristics vary along the axis. In any case, no attempt to model the shells with an optimum number of elements in both methods has been made because, the scope of the examples is to validate the proposed continuum method.

Figs. 8–11 are plotted with the circumferential axial force per unit length (cylinders) and the circumferential bending moment per unit length (cones) obtained by the application of a static radial load versus the length of the structures normalized to unit. The loads are applied on the free edges of the structures. The proposed method obtains these results performing a computation for 0 Hz. A good agreement is achieved between the results obtained with both methods. Note that in Figs. 8 and 10 (cylinder and cone 1), the effects are damped earlier than

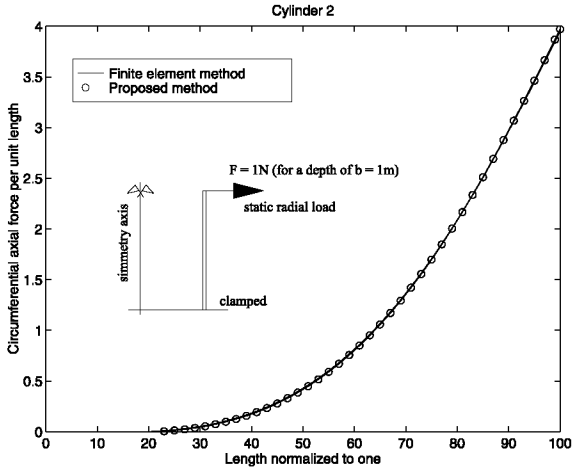

Fig. 9. Validation examples for cylinder 2 and circumferential axial force per unit length and static radial load.

in Figs. 9 and 11 (cylinder and cone 2) which means that the part of the structure that is affected by the excitation depends on the length of the structure.

3.2. *Influence of the radius of curvature*

The modal shapes of a beam on elastic foundation are the same as those of the beam. The foundation does not affect the modal shape, but it increases the frequency of the mode. The natural frequencies of the beam on elastic foundation and the beam are related by a factor that depends on the stiffness of the foundation and on the number of the considered mode. For higher modes, this factor tends to 1 and the frequencies of both beams tend to be the same.

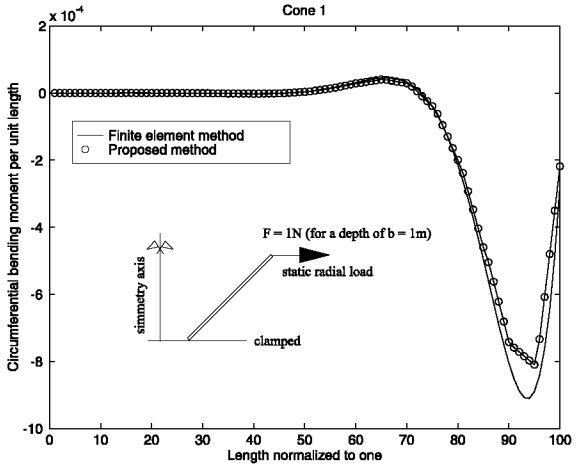

Fig. 10. Validation examples for cone 1 and circumferential bending moment per unit length and static radial load.

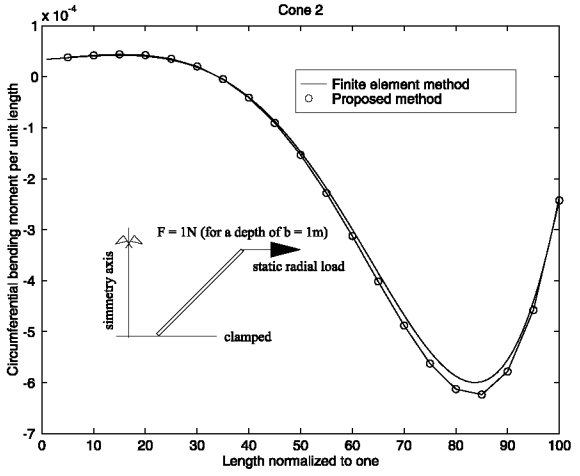

Fig. 11. Validation examples for cone 2 and circumferential bending moment per unit length and static radial load.

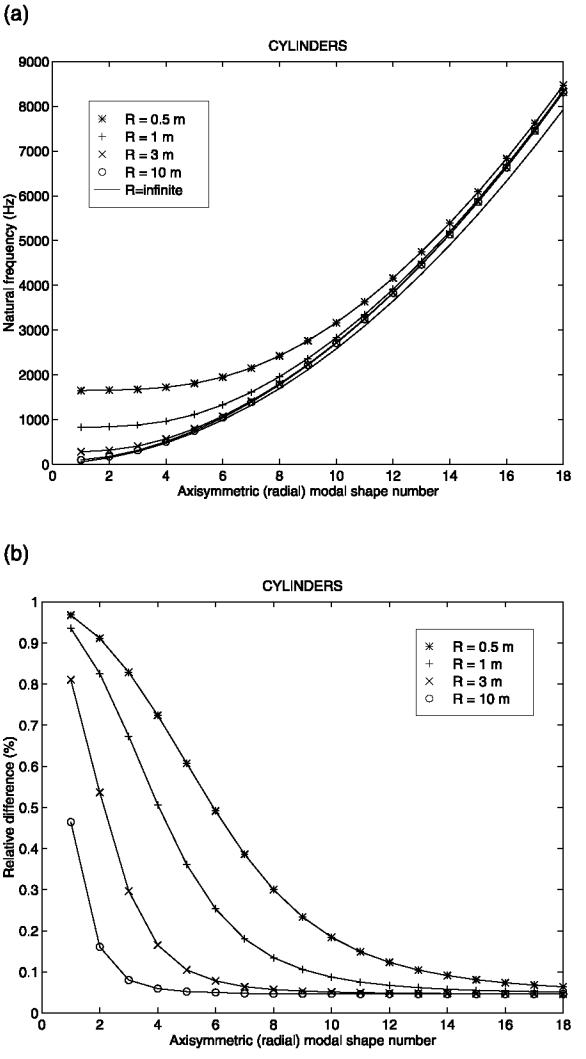

Fig. 12. Influence of the radius of curvature and results for cylinders and radial modes: (a) natural frequencies versus modal shape number, (b) relative difference versus modal shape number.

In this section, the influence of the radius of curvature is analyzed for cylindrical and conical structures. Natural frequencies of axisymmetric (radial) modes of free–free shells with different radii have been computed with the finite element method. These results are compared with the natural frequencies of a structure of infinite radius, i.e. a plane structure.

The characteristics of the cylinders are: height $h = 1$ m, thickness $t = 1 \times 10^{-2}$ m, elastic modulus $E = 2.1 \times 10^{11}$ N/m^2, Poisson's coefficient $v = 0.3$ and density $\rho = 7800$ kg/m^3. The studied radii are $R = 0.5$, 1, 3 and 10 m. The radii for the cones are the following: $R_{\min} = 0.5$, 1, 3 and 10 m, $R_{\max} = 1.5$, 2, 4 and 11 m.

The results for cylinders are shown in Fig. 12. In Fig. 12(a), natural frequencies versus modal shape number are plotted. Note that all curves tend to converge to the curve corresponding to the plane case (infinite radius). In Fig. 12(b), equivalent results are presented but in terms of relative difference, defined as $(f_R - f_{R=\infty}/f_{R=\infty})$, where f_R corresponds to the natural frequency, for a given modal shape, of a cylinder of radius R and $f_{R=\infty}$ the natural frequency of the cylinder of infinite radius. Note that when convergence occurs, the difference with the plane case is less than 10%. In Fig. 13(a) and (b), similar results are shown for conical structures.

The values of frequency when the relative difference is less than 10% for all cases are shown in Table 4.

For example, for the cone of $R_{\min} = 1$ m and $R_{\max} = 2$ m, the frequency from which the cone behaves

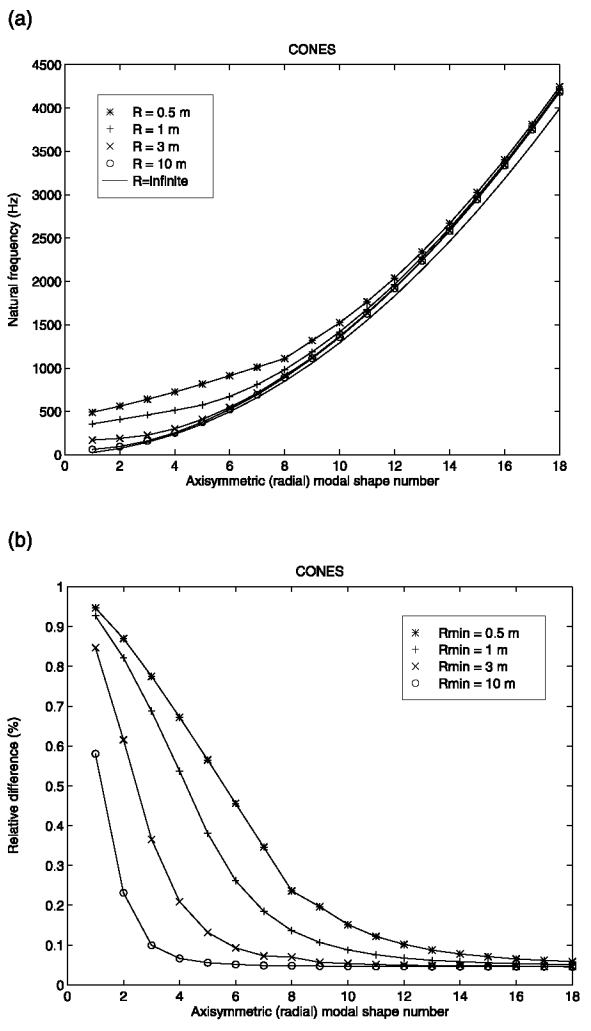

Fig. 13. Influence of the radius of curvature and results for cones. Radial modes: (a) natural frequencies versus modal shape number, (b) relative difference versus modal shape number.

practically like a plane structure is 1418 Hz (mode number 10). This means that it is enough to discretize the cone to predict this value. Above this frequency, a plane case is recovered, and the discretization does not depend on the analyzed frequency that is the main advantage of the proposed method.

3.3. Behavior for high frequency excitations

In this section, some ideas about the analysis of structures subjected to high frequency excitations with the proposed method are given. Let us take the case of a cylindrical structure in clamped-free boundary conditions. With the finite element method, some discretization is needed. The shape of axisymmetric (radial) modes has a series of waves in the axial direction. To capture one halfwave, at least two elements are necessary. So, to capture n halfwaves, the finite element mesh should have at least $2n$ elements.

Two different cylinders have been studied: Cylinder 3 ($h = 1$ m) and Cylinder 4 ($h = 0.2$ m). For both shells, the other data are $t = 1 \times 10^{-2}$ m, $E = 2.1 \times 10^{11}$ N/m^2, $\nu = 0.3$ and $\rho = 7800$ kg/m^3. In Table 5, the number of halfwaves for different radial modes and their corresponding frequency are shown. Also, the minimum number of elements needed to capture these modes with the finite element method are indicated.

This means that to analyze the dynamic behavior of cylinders 3 and 4 in the range from 0 to 60 000 Hz, at least 100 and 20 finite elements are needed, respectively. For higher ranges, this discretization is no longer valid, and a finer mesh should be used. However, with the proposed method, only one element is needed in both cases. In Figs. 14 and 15, the history of radial displacements of the free end in the frequency domain (for a step load applied in this point) are shown. For these computations, the range of frequencies has been discretized in 1024 points, i.e., the response is computed in intervals of 58.59 Hz. Note that, with the proposed method, the number of modes present in the response is independent of the discretization.

4. Conclusions

A method based on one-dimensional continuum elements to analyze orthotropic shell structures has been described. Relating the field equations of beams on elastic foundation with those of axisymmetric orthotropic shells, modeling criteria to represent shells by means of one-dimensional continuum elements have been established. The main advantage of the method is that the exact solution of the one-dimensional continuum

Table 4
Frequency values for convergence between structures of finite and infinite radii

	Cylinders				Cones			
R_{min} (m)	0.5	1	3	10	0.5	1	3	10
R_{max} (m)	0.5	1	3	10	1.5	2	4	11
Modal shape number	14	9	5	3	12	10	6	3
Frequency (Hz)	5390	2364	793	312	2039	1418	547	160

Table 5
Minimum number of finite element needed to capture a certain number of halfwaves

Cylinder 3			Cylinder 4		
Halfwaves	Frequency (Hz)	Elements	Halfwaves	Frequency (Hz)	Elements
10	2828	20	2	3910	4
20	10 219	40	4	12 226	8
30	22 124	60	6	24 904	12
40	38 014	80	8	41 379	16
50	57 053	100	10	61 049	20

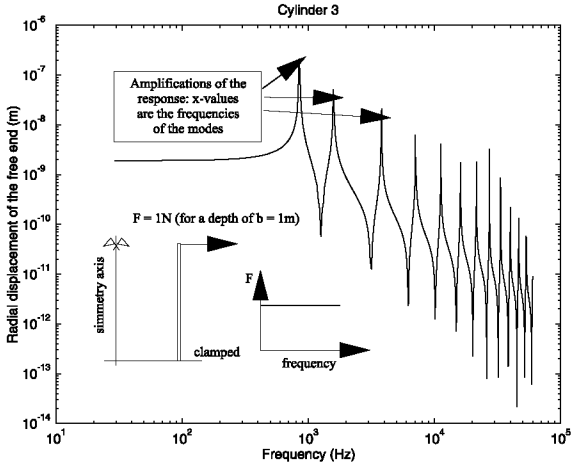

Fig. 14. Radial displacement of the free end for cylinder 3. Range of frequencies from 0 to 60 000 Hz.

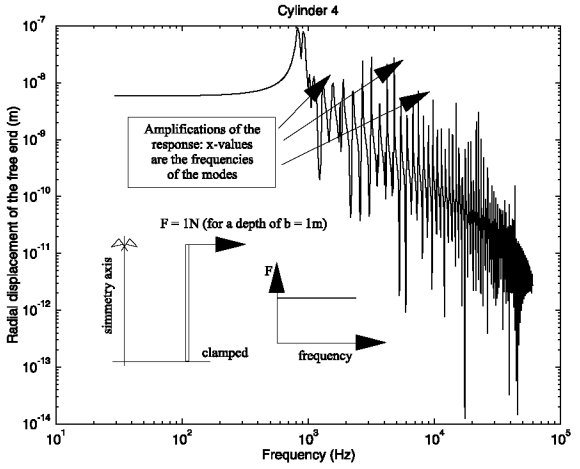

Fig. 15. Radial displacement of free end for cylinder 4. Range of frequencies from 0 to 60 000 Hz.

elements is well known in the frequency domain, and therefore, the spatial discretization of the structures is only constrained by changes in the material properties or the boundary conditions but not by the method itself. An interesting application of the method is the study of structures subjected to excitations with very high frequency contents. In these cases, methods based on spatial discretization (e.g., the finite element method) are not very convenient because they need a very fine mesh that makes any realistic computation impracticable. However, the proposed method avoids this difficulty and offers a good tool to study this kind of situations.

Some validation tests have been run to check the model. Natural frequencies of radial modes and forces per unit length due to static radial loads have been successfully compared with finite element results. The influence of the radius of curvature has been studied. The conclusion is that after a certain value of the frequency (that depends on the geometrical and material characteristics of the shell) an axisymmetric shell behaves like a plane one. This is very important for shells whose characteristics vary along the axis (for instance, conical or hyperboloidal shells) because it is only necessary to perform a discretization small enough to predict the behavior until this value of frequency. Above this value, the effect of the curvature vanishes and the shell behaves like a plane structure and the one-dimensional continuum model is valid for all values of frequency. In the last section, it is shown how, with only one continuum element, cylindrical structures can be studied in a wide range of frequencies.

Appendix A

The values of the constants a_1 to a_8 that appear in the expressions of the element impedance matrix (bending terms)

$$a_1 = 1 - \cos\lambda l \cosh\lambda l - \sin\lambda l \sinh\lambda l,$$

$$a_2 = \frac{1}{\lambda}[\cos\lambda l \sinh\lambda l - \sin\lambda l \cosh\lambda l],$$

$$a_3 = \cosh\lambda l - \cos\lambda l,$$

$$a_4 = \frac{1}{\lambda}[\sin\lambda l - \sinh\lambda l],$$

$$a_5 = -\cos\lambda l \sinh\lambda l - \sin\lambda l \cosh\lambda l,$$

$$a_6 = \frac{1}{\lambda}[\cos \lambda l \cosh \lambda l - \sin \lambda l \sinh \lambda l - 1],$$

$$a_7 = \sin \lambda l + \sinh \lambda l,$$

$$a_8 = \frac{1}{\lambda}[\cos \lambda l - \cosh \lambda l].$$

References

[1] Tin-Loi F, Pulmano A, Thambiratnam DP. Beam on elastic foundation analogy for axisymmetrically loaded cylindrical shells. Comp Struct 1990;34:281–5.

[2] Thambiratnam DP. A simple finite element analysis of hyperboloidal shell structures. Comp Struct 1993;48(2): 249–54.

[3] Thambiratnam DP, Zhuge Y. Axisymmetric free vibration analysis of conical shells. Engng Struct 1993;15(2):83–9.

[4] Akesson BA. PFVIABAT: a computer program for plane frame vibration analysis by an exact method. Int J Num Meth Engng 1976;10(6):1221–31.

[5] Kolousek V. Calcul des efforts dynamiques dans les ossatures rigides. Dunod, Paris, 1959.

[6] Huerta MC, Gómez-Lera S, Gómez-Molinero V, Solá J, Molina J, Alarcón E. Physical and mathematical modelling of wave propagation in the Ariane 5 VEB structure. Comp Struct 1990;37(2):199–205.

[7] Huerta MC, López Cela JJ, Alarcón E, Gómez Molinero V. Theoretical simulation of the Ariane 5 VEB Structure pyrotechnic shock propagation. 1ere Symp Euro Ariane 5 Struct Technol. Arcachon, France, 1993.

[8] López Cela JJ. Wave propagation in shell structures. PhD Thesis, Polytechnic University of Madrid, 1993 [in Spanish].

[9] ANSYS, Users's Manual for Revision 5.0, Swanson Analysis System Inc, 1992.